

University of Massachusetts Medical School  
**eScholarship@UMMS**

---

Thompson Lab Publications

Biochemistry and Molecular Pharmacology

---

2018-07-25


## Citrullination Inactivates Nicotinamide-N-methyltransferase

Venkatesh V. Nemmara  
*University of Massachusetts Medical School*

*Et al.*

Let us know how access to this document benefits you.

Follow this and additional works at: <https://escholarship.umassmed.edu/thompson>

 Part of the [Biochemistry Commons](#), [Enzymes and Coenzymes Commons](#), [Medicinal-Pharmaceutical Chemistry Commons](#), and the [Therapeutics Commons](#)

---

### Repository Citation

Nemmara VV, Tilwawala R, Salinger AJ, Miller L, Nguyen S, Weerapana E, Thompson PR. (2018). Citrullination Inactivates Nicotinamide-N-methyltransferase. Thompson Lab Publications. <https://doi.org/10.1021/acscchembio.8b00578>. Retrieved from <https://escholarship.umassmed.edu/thompson/117>

This material is brought to you by eScholarship@UMMS. It has been accepted for inclusion in Thompson Lab Publications by an authorized administrator of eScholarship@UMMS. For more information, please contact [Lisa.Palmer@umassmed.edu](mailto:Lisa.Palmer@umassmed.edu).

## Citrullination Inactivates Nicotinamide-N-methyltransferase

Venkatesh V Nemmara, Ronak Tilvawala, Ari J Salinger, Lacey Miller,  
Son Hong Nguyen, Eranthie Weerapana, and Paul R. Thompson

ACS Chem. Biol., **Just Accepted Manuscript** • DOI: 10.1021/acscchembio.8b00578 • Publication Date (Web): 25 Jul 2018

Downloaded from <http://pubs.acs.org> on July 27, 2018

### Just Accepted

“Just Accepted” manuscripts have been peer-reviewed and accepted for publication. They are posted online prior to technical editing, formatting for publication and author proofing. The American Chemical Society provides “Just Accepted” as a service to the research community to expedite the dissemination of scientific material as soon as possible after acceptance. “Just Accepted” manuscripts appear in full in PDF format accompanied by an HTML abstract. “Just Accepted” manuscripts have been fully peer reviewed, but should not be considered the official version of record. They are citable by the Digital Object Identifier (DOI®). “Just Accepted” is an optional service offered to authors. Therefore, the “Just Accepted” Web site may not include all articles that will be published in the journal. After a manuscript is technically edited and formatted, it will be removed from the “Just Accepted” Web site and published as an ASAP article. Note that technical editing may introduce minor changes to the manuscript text and/or graphics which could affect content, and all legal disclaimers and ethical guidelines that apply to the journal pertain. ACS cannot be held responsible for errors or consequences arising from the use of information contained in these “Just Accepted” manuscripts.



## Citrullination Inactivates Nicotinamide-*N*-methyltransferase

Venkatesh V. Nemmara<sup>1,2</sup>, Ronak Tilvawala<sup>1,2</sup>, Ari J. Salinger<sup>1,2</sup>, Lacey Miller<sup>1</sup>, Son Hong Nguyen<sup>1,2</sup>, Eranthie Weerapana<sup>3</sup>, and Paul R. Thompson<sup>1,2\*</sup>

<sup>1</sup>Department of Biochemistry and Molecular Pharmacology, UMass Medical School, 364 Plantation Street, Worcester, MA 01605, USA

<sup>2</sup>Program in Chemical Biology, UMass Medical School, 364 Plantation Street, Worcester, MA, 01605, USA.

<sup>3</sup>Department of Chemistry, Boston College, Chestnut Hill, MA 02467

Running Title: Citrullination Inactivates NNMT

\* Author to whom correspondence should be addressed: Department of Biochemistry and Molecular Pharmacology, University of Massachusetts Medical School, LRB 826, 364 Plantation Street, Worcester MA 01605 tel: 508-856-8492; fax: 508-856-6215; e-mail: paul.thompson@umassmed.edu.

## Abstract

Nicotinamide-*N*-methyl transferase (NNMT) catalyzes the irreversible methylation of nicotinamide (NAM) to form *N*-methyl nicotinamide (MeNAM) using SAM as a methyl donor. NNMT is implicated in several chronic disease conditions, including cancers, kidney disease, cardiovascular disease, and Parkinson's disease. Although phosphorylation of NNMT in gastric tumors is reported, the functional effects of this post-translational modification has not been investigated. We previously reported that citrullination of NNMT by Protein Arginine Deiminases (PADs) abolished its methyltransferase activity. Herein, we investigate the mechanism of inactivation. Using tandem MS, we identified three sites of citrullination in NNMT. With this information in hand, we used a combination of site-directed mutagenesis, kinetics, and CD experiments to demonstrate that citrullination of R132 leads to a structural perturbation that ultimately promotes NNMT inactivation.

## INTRODUCTION

Nicotinamide-*N*-methyl transferase (NNMT) is a cytosolic enzyme that uses *S*-adenosyl methionine (SAM) as a cofactor to catalyze the *N*-methylation of nictotinamide (NAM) to form *N*-methyl nicotinamide (MeNAM) (Figure 1A).<sup>1,2</sup> NNMT is predominantly expressed in the liver and is also present in kidney, brain, lung, adipose tissues, and muscle.<sup>1,3-6</sup> NNMT regulates the intracellular levels of SAM and NAM in the methionine cycle and nicotinamide adenine dinucleotide (NAD<sup>+</sup>) synthesis pathways, which are crucial controls of cellular energy expenditure.<sup>4,7</sup> Notably, NNMT is overexpressed in a variety of cancers and metabolic conditions. For example, aberrant NNMT expression is observed in papillary thyroid,<sup>8,9</sup> gastric,<sup>10</sup> oral, and renal carcinoma,<sup>11,12</sup> as well as adenocarcinoma,<sup>13,14</sup> glioblastoma,<sup>15</sup> bladder,<sup>15</sup> colorectal,<sup>16</sup> and lung cancers.<sup>17</sup> Furthermore, increased NNMT expression has been found in the lumbar spinal fluids of patients with Parkinson's disease suggesting a potential role in neurodegenerative diseases.<sup>18,19</sup> ASO treatment shows efficacy in metabolic diseases confirming the therapeutic potential of targeting this enzyme.<sup>20</sup>

Increased NNMT activity has been shown to regulate the methylation potential in cancer cells by altering SAM and *S*-adenosylhomocysteine (SAH) concentrations.<sup>21</sup> Despite recent advances, NNMT regulation in cancers and other metabolic disorders like diabetes, remains poorly understood. Many enzymes undergo post-translational modifications and the activity of a clear majority of them are regulated through these modifications.<sup>22,23</sup> Post-translational modification of NNMT was first reported by Lim *et al.*<sup>24</sup> The authors showed that NNMT is phosphorylated in gastric tumors and demonstrated that casein kinase 2 efficiently phosphorylates recombinant NNMT. However, the mechanism and impact of such a modification was not explored.

1  
2  
3 Our recent proteomic datasets revealed that NNMT is citrullinated in synovial tissue  
4 samples obtained from patients with rheumatoid arthritis (RA).<sup>25</sup> Citrullination is a post-  
5 translational modification wherein a peptidyl-arginine is hydrolyzed to form peptidyl-citrulline  
6 (Figure 1B).<sup>26, 27</sup> This deimination reaction is catalyzed by the calcium dependent Protein  
7 Arginine Deiminases (PADs).<sup>26, 27</sup> The PAD superfamily includes five mammalian isozymes,  
8 PADs 1-4 and 6. Of these enzymes, PADs 1-4 have deiminase activity whereas PAD6 is  
9 catalytically inactive due to various mutations.<sup>26</sup> Although highly related, PADs display unique  
10 cellular and tissue distribution patterns throughout the body.<sup>26-29</sup> Specifically, PAD1 and PAD3  
11 are principally expressed in skin and hair follicles,<sup>28</sup> PAD2 and PAD4 are expressed in  
12 neutrophils and myeloid cells<sup>26, 30</sup> and PAD6 is expressed in oocytes and embryos.<sup>31, 32</sup> PADs  
13 citrullinate numerous proteins including filaggrin, keratin, and vimentin.<sup>33</sup> In addition, PAD1  
14 has been shown to promote tumorigenesis by regulating MEK1-ERK1/2-MMP2 signaling in  
15 triple negative breast cancer.<sup>34</sup> PAD2 is upregulated in multiple sclerosis and in breast  
16 cancers.<sup>35, 36</sup> PAD2 is also released into the synovial joints of patients with RA, leading to the  
17 citrullination of multiple protein targets, which promotes the generation of anti-citrullinated  
18 protein antibodies (ACPA), a characteristic feature of RA.<sup>37, 38</sup>

19  
20  
21 Since abnormal PAD activity is associated with a variety of autoimmune diseases,  
22 including RA, ulcerative colitis, lupus, and multiple sclerosis as well as various cancers,<sup>30, 31</sup> the  
23 PADs are potential therapeutic targets.<sup>39, 40</sup> We recently demonstrated that citrullination of  
24 Serine Protease Inhibitors (SERPIN) can abolish their ability to inhibit their cognate proteases.<sup>25</sup>  
25 We also established that NNMT citrullination abolished its methyltransferase activity.<sup>25</sup> Here,  
26 we report a detailed analysis of NNMT citrullination by PAD1 and PAD2 and its effect on  
27  
28  
29  
30  
31  
32  
33  
34  
35  
36  
37  
38  
39  
40  
41  
42  
43  
44  
45  
46  
47  
48  
49  
50  
51  
52  
53  
54  
55  
56  
57  
58  
59  
60

1  
2  
3 NNMT structure and function. Specifically, we show that citrullination destabilizes the protein,  
4  
5 which ultimately leads to NNMT inactivation.  
6  
7  
8  
9  
10  
11  
12  
13  
14  
15  
16  
17  
18  
19  
20  
21  
22  
23  
24  
25  
26  
27  
28  
29  
30  
31  
32  
33  
34  
35  
36  
37  
38  
39  
40  
41  
42  
43  
44  
45  
46  
47  
48  
49  
50  
51  
52  
53  
54  
55  
56  
57  
58  
59  
60

## RESULTS AND DISCUSSION

### Effect of citrullination on the methyl transferase activity of NNMT.

Our previous study showed that citrullination of NNMT by PAD1 and PAD2 completely abolished its methyltransferase activity when either SAM or quinoline were evaluated as the varied substrates (Figure 1C).<sup>25</sup> By contrast, citrullination of NNMT by either PAD3 or PAD4 only led to a moderate reduction in activity. Note that NNMT activity was measured using the alternative substrate quinoline (Figure S1A)<sup>41</sup> and monitoring the formation of 1-methylquinolinium by fluorescence (Figure S1B).<sup>42</sup>

To gain insights into the mechanism of NNMT inactivation, we first determined the steady-state kinetic parameters for PAD mediated citrullination. To identify optimal assay conditions, we first citrullinated wild type NNMT with increasing concentrations of PAD1 and PAD2. The extent of citrullination was determined by rhodamine phenylglyoxal (Rh-PG) labeling (Figure S2A).<sup>43</sup> Next, we generated progress curves of NNMT citrullination to identify the linear range of PAD activity (Figure 2A and B). Subsequently, we measured the initial rates for the citrullination of NNMT (Figure 2C and D). Note that a standard curve was generated to convert the fluorescence intensity of Rh-PG into citrulline concentration (Figure S3A and B).<sup>43</sup> From these experiments, we obtained  $k_{\text{cat}}/K_m$  values of  $4600 \text{ M}^{-1}\text{s}^{-1}$  and  $3500 \text{ M}^{-1}\text{s}^{-1}$  for PAD1 and PAD2 respectively. Although these values are comparable to other known substrates, e.g., histone H3 ( $k_{\text{cat}}/K_m = 4800 \text{ M}^{-1}\text{s}^{-1}$ ) and BAEE ( $k_{\text{cat}}/K_m = 1500 \text{ M}^{-1}\text{s}^{-1}$ ), it should be noted that the  $k_{\text{cat}}$  and  $K_m$  values for PAD1 ( $k_{\text{cat}} = 0.014 \pm 0.01 \text{ s}^{-1}$ ;  $K_m = 3.0 \pm 0.8 \text{ }\mu\text{M}$ ) and PAD2 ( $k_{\text{cat}} = 0.007 \pm 0.002 \text{ s}^{-1}$ ;  $K_m = 2.0 \pm 0.1 \text{ }\mu\text{M}$ ) are 50- to 100-fold lower than typically observed;<sup>43, 44</sup> the lower  $K_m$  value compensates for the decreased  $k_{\text{cat}}$  such that  $k_{\text{cat}}/K_m$  values are similar. Given that PADs citrullinate NNMT in a time-dependent manner and citrullination abolishes its methyltransferase



1  
2  
3 activity, we next investigated the dose dependent inactivation of NNMT by PAD1 and PAD2  
4 (Figure S2B). From these experiments we obtained IC<sub>50</sub> values of 0.25 μM for PAD1 and 0.8  
5  
6 μM for PAD2 suggesting that both PAD1 and PAD2 inactivate NNMT in a concentration  
7  
8 dependent manner.  
9  
10

### 11 12 13 **Identification of citrullination sites in NNMT.** 14 15

16 Having established that citrullination abolishes NNMT activity, we then identified the  
17 sites of citrullination in NNMT. Since protein citrullination increases the mass of a peptide  
18 fragment by only 0.98 Da, it is difficult to unambiguously identify citrullination sites in a  
19 protein.<sup>45</sup> Therefore, we employed a novel chemical labeling approach to identify the  
20 citrullination sites in NNMT. For these experiments, we citrullinated NNMT and then labeled  
21 the protein with phenylglyoxal (PG). PG selectively modifies citrullinated residues under acidic  
22 conditions<sup>46, 47</sup> and the modified peptides show a mass increase of 117 Da (Figure 3A). PG  
23 modified sites can therefore be unambiguously interpreted as citrullination sites. We used  
24 Neutrophil Elastase (NE) for peptide digestion instead of the commonly used Trypsin. Trypsin  
25 cleaves peptides after arginine and lysine residues, but generally not after citrulline residues. By  
26 contrast, NE cleaves after alanine and valine residues thereby making it an optimal choice for  
27 peptide digestion. NE digested peptides were then subjected to chromatography coupled with  
28 tandem mass spectrometry analysis. Sequence coverage of NNMT was 85%, and included all  
29 nine arginine residues in the protein.  
30  
31  
32  
33  
34  
35  
36  
37  
38  
39  
40  
41  
42  
43  
44  
45  
46  
47  
48

49 The proteomic data identified three PG modified peptide fragments. Figure 3B shows the  
50 sequence of these peptide fragments with PG-modified citrulline residues at positions R18, R132  
51 and R181. The corresponding arginine residues in the control sample did not show a mass  
52  
53  
54  
55  
56  
57  
58  
59  
60

1  
2  
3 change of +117.0102 Da. Figure 3C depicts a representative high-resolution MS/MS spectrum  
4  
5 for the citrullination of R132 that unambiguously confirmed PG modification of this residue.  
6  
7

### 8 **Determining the role of citrullinated residues in NNMT.**

9

10  
11 To probe the role of citrullinated residues in abolishing NNMT activity, we generated  
12  
13 constructs encoding arginine to lysine residues for all nine arginines in NNMT (Figure 4A). We  
14  
15 expressed and purified all mutant enzymes and analyzed their methyltransferase activity.  
16  
17 Interestingly, all mutants except R132K showed comparable methyltransferase activity to that of  
18  
19 wild type NNMT. As depicted in Figure 4B, R132K exhibits a 5-fold reduction in the  $k_{cat}/K_m$   
20  
21 value for both SAM and quinoline. Next, we confirmed that these NNMT mutants are also PAD  
22  
23 substrates by treating them with PAD1 or PAD2 followed by labeling with Rh-PG. As depicted  
24  
25 in Figure S4, all NNMT mutants showed efficient citrullination by PADs 1 and 2. These data are  
26  
27 consistent with our findings that at least three residues in NNMT can be citrullinated.  
28  
29  
30  
31

32  
33 Given that PADs efficiently citrullinate both wild type NNMT and mutant enzymes, we  
34  
35 examined the effect of citrullination on the methyltransferase activity of the NNMT mutants.  
36  
37 Mutants were citrullinated with either PAD1 or PAD2 and their methyltransferase activity was  
38  
39 measured and compared with the uncitrullinated controls treated under the same condition  
40  
41 (Figures 4C, 4D, S5, and S6 and Tables S1 and S2). All of the uncitrullinated arginine mutants,  
42  
43 except R132K, retained  $\geq 80\%$  of their methyltransferase activity. Uncitrullinated R132K, like  
44  
45 its citrullinated counterpart, lost its methyltransferase activity. R132 is one of the citrullination  
46  
47 sites identified in our mass spectrometric dataset along with R18 and R181. It is interesting to  
48  
49 note that uncitrullinated R18K and R181K did not lose their methyltransferase activity. This  
50  
51 data suggests that R132 is essential for the methyltransferase activity of NNMT.  
52  
53  
54  
55  
56  
57  
58  
59  
60

1  
2  
3 Next, we determined the rate of inactivation of citrullinated R18K, R132K and R181K  
4 and compared them with their uncitrullinated controls (Figures 4E, 4 F, and S7). We  
5 hypothesized that if R132 is the only residue responsible for the loss of NNMT activity upon  
6 citrullination, then the rate of inactivation of uncitrullinated and citrullinated R132K will remain  
7 the same. Indeed, the obtained rate constants of inactivation for citrullinated ( $k = 0.01 \text{ s}^{-1}$ ) and  
8 uncitrullinated ( $k = 0.012 \text{ s}^{-1}$ ) R132K mutant are quite similar. In stark contrast, the rates of  
9 inactivation of citrullinated R18K and R181K are roughly 10-fold higher than the uncitrullinated  
10 controls (Figures 4F, and Table 1). Taken together, these results clearly demonstrate that despite  
11 multiple sites of citrullination, modification of R132 leads to NNMT inactivation.  
12  
13  
14  
15  
16  
17  
18  
19  
20  
21  
22  
23

### 24 **Structural basis of inactivation.**

25  
26  
27 To gain insights into the structural role of R132, we analyzed the crystal structure of  
28 NNMT (PDB ID: 3ROD). NNMT is a class-I SAM dependent methyltransferase comprised of a  
29 seven-stranded  $\beta$ -sheet flanked by eight  $\alpha$ -helices on both sides that are connected by ten  
30 loops.<sup>48-50</sup> The ternary complex of NNMT bound to its substrate NAM and *S*-adenosyl  
31 homocysteine (SAH)<sup>51</sup> shows that the adenine ring of SAH makes hydrophobic interactions with  
32 the sidechains of Y86 from helix-4 and A169 from helix-7 (Figures 5 and S8). Moreover, it also  
33 makes hydrogen bonding interactions with the sidechain of D142 and the backbone amide of  
34 V143 (Figure S8), which are anchored on loop-7.<sup>51</sup> Molecular dynamics simulations on the  
35 NNMT mutant D197A suggested that loop-7, which is formed by residues V138-L154,  
36 undergoes a major conformational change relative to wildtype. Such a change results in  
37 decreased binding of SAH to the mutant enzyme.<sup>51</sup> As shown in Figure 5A, loop -7 is connected  
38 to helix-6 through a  $\beta$ -strand. Notably, R132 from helix-6 interacts with E128 and E129 of the  
39 same helix via electrostatic interactions. R132 also makes a cationic- $\pi$  interaction with the  
40  
41  
42  
43  
44  
45  
46  
47  
48  
49  
50  
51  
52  
53  
54  
55  
56  
57  
58  
59  
60

1  
2  
3 indole ring of W97 from helix-4. (Figure 5B). Additionally, the  $\epsilon$ -nitrogen of R132 hydrogen  
4 bonds with the backbone carbonyl oxygen of W97. These interactions exhibited by the positively  
5 charged R132 with helix-4 are important because any disruption would likely result in a  
6 structural perturbation. Such a structural perturbation would destabilize loop-7, which would be  
7 expected to impact SAM binding. Furthermore, the loss of an interaction between helix-4 and  
8 helix-6 could in turn disrupt interactions of residues Y86 and S87 with SAM (Figure S8). Taken  
9 together, these data suggest that citrullination of R132 destabilizes NNMT, which subsequently  
10 leads to enzyme inactivation.  
11  
12  
13  
14  
15  
16  
17  
18  
19  
20  
21

22 Consistent with this hypothesis is the fact that the rate of inactivation of the R132K  
23 mutant with and without a PAD are nearly identical. The lysine mutant is intrinsically  
24 destabilized due to the inability of a lysine to fully substitute for the network of interactions  
25 afforded by R132. Based on these observations, it is likely that the methyltransferase activity of  
26 citrullinated NNMT is abolished due to structural perturbations resulting from the loss of  
27 positive charge on R132. To further confirm this hypothesis, we generated alanine (R132A) and  
28 glutamine (R132Q) mutants. Interestingly, neither of these mutants were found in soluble  
29 fractions. In addition, the insoluble fractions did not possess methyltransferase activity (Figure  
30 S9), suggesting that R132 is important residue for folding and for maintaining the secondary  
31 structure of the protein.  
32  
33  
34  
35  
36  
37  
38  
39  
40  
41  
42  
43  
44  
45

46 To further probe the role of R132 in maintaining the secondary structure of NNMT we  
47 used circular dichroism (CD) spectroscopy. For these studies we measured the far UV CD-  
48 spectra of wild type NNMT under three different conditions: without incubation, and incubated  
49 at 37 °C in the presence and absence of PAD1. The spectrum of wild type NNMT by itself has  
50 strong minima at 230 nm, which do not change significantly for the uncitrullinated enzyme  
51  
52  
53  
54  
55  
56  
57

1  
2  
3 incubated at 37 °C. However, citrullinated NNMT show a 30% reduction in the molar ellipticity  
4 at 230 nm (Figure 5C). This result indicates that the secondary structure of the citrullinated  
5 enzyme is perturbed upon citrullination. We also carried out the same experiments with the  
6 R132K mutant (Figure 5D). The mutant enzyme without incubation displayed strong minima at  
7 230 nm with 90% of the ellipticity of the wild type enzyme. The uncitrullinated and citrullinated  
8 mutant incubated in the absence and presence of PAD1 showed a decrease in molar ellipticity at  
9 230 nm by 40% and 38%, respectively. These results are also consistent with the hypothesis that  
10 citrullination destabilizes the protein leading to its inactivation.  
11  
12  
13  
14  
15  
16  
17  
18  
19  
20  
21

## 22 **Conclusions.**

23  
24  
25 In summary, we report that NNMT activity is regulated by citrullination. Using tandem  
26 mass spectrometry along with site-directed mutagenesis and kinetics, we explored the detailed  
27 mechanism of inactivation of citrullinated NNMT. Mass spectrometry experiments identified  
28 three citrullination sites in NNMT, of which, R132 was found to be essential for maintaining  
29 NNMT activity. Furthermore, CD experiments revealed that citrullination results in a structural  
30 perturbation of NNMT. Although we cannot definitively rule out an effect on cofactor binding,  
31 citrullination of the R132K mutant does not enhance its rate of inactivation, which indicates that  
32 the loss of activity is due to the loss of an optimized interaction. Moreover, the R132K mutation  
33 does not affect the  $K_m$  for SAM. Therefore, we conclude that R132 citrullination results in the  
34 loss of crucial interactions that maintain the structural integrity of NNMT. Taken together, these  
35 data indicate that R132 citrullination lights a fuse that ultimately leads to NNMT inactivation via  
36 a loss in structural integrity. NNMT is overexpressed in numerous cancers and high levels are  
37 known to alter the SAM/SAH ratio in cells, which can have profound effects on DNA and  
38 histone methylation. Notably, a recent study showed that NNMT overexpression promotes a  
39  
40  
41  
42  
43  
44  
45  
46  
47  
48  
49  
50  
51  
52  
53  
54  
55  
56  
57  
58  
59  
60

1  
2  
3 pro-growth phenotype.<sup>21</sup> Since citrullination abolishes NNMT activity, the PADs may  
4  
5 downregulate NNMT activity in a subset of tumors. Consistent with that possibility is the fact  
6  
7 that PAD2 act as a tumor suppressor in a subset of breast cancers.<sup>52</sup> Overall, these results  
8  
9 provide insights into the regulation of NNMT activity via citrullination under physiological  
10  
11 conditions.  
12  
13  
14  
15  
16  
17  
18  
19  
20  
21  
22  
23  
24  
25  
26  
27  
28  
29  
30  
31  
32  
33  
34  
35  
36  
37  
38  
39  
40  
41  
42  
43  
44  
45  
46  
47  
48  
49  
50  
51  
52  
53  
54  
55  
56  
57  
58  
59  
60

## METHODS

**Materials.** PADs 1, 2, 3 and 4 were purified as reported.<sup>44, 53</sup> Rhodamine-phenylglyoxal (Rh-PG) was synthesized as reported.<sup>43</sup> The plasmid pET28a-LIC, harboring the *NNMT* gene was purchased from Addgene (Addgene plasmid # 40734). All chemicals were purchased from Sigma.

### Site-directed mutagenesis.

The pET28:NNMT vector was used as a template for generating all arginine to lysine mutations. Primers used for mutating the individual arginine residues are shown in Table S3. PCR reactions were performed under standard conditions using the respective primers along with *iProof* high-fidelity DNA polymerase (*BIO-RAD*) in GC buffer and dNTPs in the reaction mixture. The PCR product was analyzed on a 1% (w/v) agarose gel and the amplification product was incubated with 10 units of Dpn1 for 2 h at 37 °C. The product was then transformed into *E. coli* BL21(DE3) host cells and single colonies were selected. DNA sequencing of the insert gene confirmed the desired mutation. Expression and purification of the mutants were performed as described for the wild-type enzyme (see below).

### Purification of recombinant human NNMT.

Human NNMT was purified using the methodology outlined below. Briefly, a pET28 vector encoding human NNMT was transformed into BL21(DE3) cells and grown in 2 L of Terrific Broth (TB) containing 50 µg/mL of kanamycin to an OD of 0.6-0.8 at 37 °C diluted 1:10 from an overnight culture. Protein expression was induced with 1.0 mM IPTG for 16-18 h at 16 °C. The cells were pelleted by centrifugation, resuspended in lysis buffer (50 mM Tris pH 8.0, 300 mM NaCl, 5 mM imidazole, 2 mM β-mercaptoethanol, 1 mM PMSF) before sonication.

1  
2  
3 The lysate was centrifuged and the supernatant containing soluble NNMT was incubated with  
4 Ni-NTA resin (GE biosciences). The resin was washed twice with lysis buffer containing 30  
5 mM and 70 mM of imidazole, respectively, and the protein was eluted with 250 mM of  
6 imidazole. The protein was further dialyzed overnight at 4 °C in dialysis buffer (50 mM Tris pH  
7 8.0, 300 mM NaCl, 5% glycerol, and 1 mM DTT) to remove imidazole. The dialyzed fractions  
8 were concentrated to obtain 4 mg/mL protein aliquots and were flash frozen using liquid  
9 nitrogen. The Bradford assay was used to determine protein concentrations.  
10  
11  
12  
13  
14  
15  
16  
17  
18  
19  
20  
21

### 22 **Human NNMT activity assay.**

23  
24 Human NNMT activity assays were carried out in two different scenarios using quinoline  
25 as the substrate and SAM as the coenzyme. To measure NNMT activity against quinoline,  
26 citrullinated and uncitrullinated NNMT were added to individual wells of a 96-well plate (final  
27 concentration 0.6 μM (60 μL) containing various quinoline concentrations (0, 10, 20, 40, 60, and  
28 80, and 100 μM) and a fixed SAM concentration (100 μM). The assay contained buffer  
29 composed of 5 mM Tris pH 8.6 and 1 mM DTT. To measure NNMT activity against SAM,  
30 citrullinated and uncitrullinated NNMT were added to individual wells of a 96-well plate (final  
31 concentration 0.6 μM, 60 μL) containing various SAM concentrations (0, 10, 20, 40, 60, and  
32 100, and 140 μM) and a fixed quinoline concentration (100 μM) in assay. The initial velocity  
33 proportional to enzymatic activity was measured by monitoring the formation of 1-  
34 methylquinolinium fluorometrically ( $\lambda_{ex} = 330$  nm;  $\lambda_{em} = 405$  nm). The initial rates obtained  
35 from these assays were fit by nonlinear least fit squares to equation 1,  
36  
37  
38  
39  
40  
41  
42  
43  
44  
45  
46  
47  
48  
49  
50

$$51 \quad v = V_{\max}[S]/ K_M + [S] \quad \text{Eq 1,}$$



1  
2  
3 using the GraphPad Prism 7.0 software package and kinetic parameters were calculated. The  
4  
5 experiment was carried out in duplicate.  
6  
7  
8  
9

### 10 **Detection of citrullination sites in NNMT.**

11  
12  
13 Pure NNMT was labelled with phenylglyoxal similarly to previously described methods.<sup>43</sup>  
14  
15 Briefly, NNMT (100 µg) was first citrullinated by incubating at 37 °C in 100 mM HEPES pH  
16  
17 7.6, 100 mM NaCl, 500 µM TCEP, and 1 mM CaCl<sub>2</sub> with PAD1 or PAD2 (100 µg) for 2 h. As  
18  
19 a control, NNMT was incubated under the same conditions in the absence of a PAD.  
20  
21  
22 Citrullinated proteins were then incubated with 20% trichloroacetic acid (TCA) (40 µL of 100%  
23  
24 TCA) and phenylglyoxal (250 µM) for 3 h at 37 °C. Next, the labeling reaction was quenched  
25  
26 with 25 µL of 0.5 M citrulline dissolved in 50 mM HEPES pH 7.6. The solutions were then  
27  
28 placed on ice for 30 min followed by centrifugation (13,500 rpm, 15 min) at 4 °C. The  
29  
30 supernatants were discarded, and the protein pellets were washed twice with cold acetone and  
31  
32 dried. The protein pellets were then sonicated and resolubilized in 6 M urea (30 µL) and 100 mM  
33  
34 ammonium bicarbonate (70 µL) solution. Once dissolved, the samples were incubated with 1 M  
35  
36 DTT (1.5 µL) for 15 min at 65 °C followed by incubation with 500 mM iodoacetamide (2.5 µL)  
37  
38 for 30 min at RT. After 30 min, the samples were diluted to 1 mL final volume with PBS to bring  
39  
40  
41 down the urea concentration to ~2 M. The samples were then treated with neutrophil elastase (3  
42  
43 µL, 1:20 dilution) overnight at 37 °C. The samples were dried using a speedVac and further  
44  
45 subjected to three spin column washes. The eluted samples were further dried using a speedVac,  
46  
47 resolubilized in Buffer A (95% ACN, 5 % water and 0.5 % formic acid) and stored at -20 °C  
48  
49  
50 until MS analysis.  
51  
52  
53  
54  
55  
56  
57  
58  
59  
60

### LC/LC-MS/MS and data processing.

LC-MS/MS analysis was performed on an LTQ-Orbitrap Discovery mass spectrometer (ThermoFisher) coupled to an Agilent 1200 series HPLC. Samples were loaded via HPLC autosampler onto a hand-pulled 100  $\mu\text{m}$  fused-silica capillary column with a 5  $\mu\text{m}$  tip packed with 10 cm Aqua C18 reverse phase resin (Phenomenex). Peptides were eluted over a 5 h elution using a gradient from 100% Buffer A (95% water, 5% acetonitrile, 0.1% formic acid) to 100% Buffer B (20% water, 80% acetonitrile, 0.1% formic acid). The flow rate through the column was set to  $\sim 0.25$   $\mu\text{L}/\text{min}$  and the spray voltage was set to 2.75 kV. One full MS scan was followed by 8 data dependent scans of the 8 most abundant ions. For high resolution runs, a full scan was followed by 4 data dependent scans limited to an inclusion mass list containing the masses of previously identified modified peptides. The tandem MS data were searched using the SEQUEST algorithm using a concatenated target/decoy variant of the human UniProt database. A static modification of +57.02146 on cysteine was specified to account for alkylation by iodoacetamide and a differential modification of +117.0102 was specified on arginine. SEQUEST output files were filtered using DTA-Select.

### Detection of NNMT citrullination by rhodamine-PG labeling.

Protein citrullination was carried out as described previously.<sup>46</sup> Briefly, NNMT (6  $\mu\text{M}$ ) was incubated in buffer (100 mM HEPES pH 7.6, 100 mM NaCl, 500  $\mu\text{M}$  TCEP, 1 mM  $\text{CaCl}_2$ ) with or without PAD (0, 0.125, 0.5, 1, 2, and 4  $\mu\text{M}$ ) at 37  $^\circ\text{C}$  for 2 h. The samples were then incubated with 20% TCA (10  $\mu\text{L}$  of 100% TCA) and 0.1 mM rhodamine-PG (1  $\mu\text{L}$  of 5 mM stock) for 30 min at 37  $^\circ\text{C}$ . After a 30 min incubation, the reaction was quenched with citrulline

1  
2  
3 (0.1 M final concentration) dissolved in 50 mM HEPES pH 7.6. The solutions were placed on  
4  
5 ice for 30 min followed by centrifugation (13,500 rpm, 15 min) at 4 °C. The supernatants were  
6  
7 discarded, and the protein pellets were washed twice with cold acetone and dried. To eliminate  
8  
9 arginine labeling, the pellet was dissolved in 20  $\mu$ L of buffer containing 20 mM HEPES pH 8.0,  
10  
11 100 mM arginine, 1% SDS, 7%  $\beta$ -mercapto ethanol, and 100 mM NaCl. The samples were  
12  
13 further boiled with 6X SDS loading dye and sonicated for 15 min and separated by SDS-PAGE  
14  
15 (12.5% gel). Bands were visualized by scanning the gel in a typhoon scanner (approximate  
16  
17 excitation/emission maxima ~546/579, respectively).  
18  
19  
20  
21

### 22 **Time dependent NNMT citrullination visualized by Rh-PG.**

23  
24  
25 Time dependent citrullination of NNMT was carried out by incubating NNMT (6  $\mu$ M) in buffer  
26  
27 (100 mM HEPES pH 7.6, 100 mM NaCl, 500  $\mu$ M TCEP, 1 mM  $\text{CaCl}_2$ ) with or without a PAD  
28  
29 (final concentration 0.7  $\mu$ M) at 37 °C for various time intervals (0, 15, 30, 45, 60, 75, 90, 105,  
30  
31 and 120 min) and flash frozen to stop the reaction. The samples were then incubated with 20%  
32  
33 TCA (10  $\mu$ L of 100% TCA) and 0.1 mM rhodamine-PG (1  $\mu$ L of 5 mM stock) for 30 min at 37  
34  
35 °C. After a 30 min incubation, the reaction was quenched with 10  $\mu$ L of 0.5 M citrulline  
36  
37 dissolved in 50 mM HEPES pH 7.6. The solutions were placed on ice for 30 min followed by  
38  
39 centrifugation (13,500 rpm, 15 min) at 4 °C. The supernatants were discarded, and the protein  
40  
41 pellets were washed twice with cold acetone and dried. To eliminate arginine labeling, the pellet  
42  
43 was dissolved in 20  $\mu$ L of buffer containing 20 mM HEPES pH 8.0, 100 mM arginine, 1% SDS,  
44  
45 7%  $\beta$ -mercapto ethanol, and 100 mM NaCl. The samples were further boiled with 6X SDS  
46  
47 loading dye and sonicated for 15 min and separated by SDS-PAGE (12.5% gel). Bands were  
48  
49 visualized by scanning the gel in a typhoon scanner (approximate excitation/emission maxima  
50  
51  
52  
53  
54  
55  
56  
57  
58  
59  
60

1  
2  
3 ~546/579, respectively). The experiment was carried out in duplicate, the band intensities were  
4  
5 quantified and the data were fit to equation 2, using GraphPad Prism 7.0 software package.  
6  
7

$$F = F_0 (1 - e^{-kt}) \quad \text{Eq 2,}$$

11  
12  
13  $F$  is the normalized fluorescence intensity and  $F_0$  is the normalized fluorescence intensity at time  
14  
15 zero.  $k$  is the pseudo-first order rate constant of NNMT citrullination by PADs and  $t$  is time.  
16  
17

### 18 **NNMT inactivation as a function of PAD concentration.**

19  
20  
21 NNMT (6  $\mu\text{M}$ ) was incubated in buffer (100 mM HEPES pH 7.6, 100 mM NaCl, 500  
22  
23  $\mu\text{M}$  TCEP, 1 mM  $\text{CaCl}_2$ ) with or without a PAD (0, 0.125, 0.5, 1, 2, and 4  $\mu\text{M}$ ) at 37  $^\circ\text{C}$  for 2 h.  
24  
25 Methyltransferase activity was evaluated with PAD-treated NNMT as described above. The  
26  
27 experiment was carried out in duplicate. The  $\text{IC}_{50}$  values were then determined by fitting the  
28  
29 activity data to equation 3,  
30  
31

$$\text{Percent activity} = 100 / (1 + [\text{I}] / \text{IC}_{50}) \quad \text{Eq 3,}$$

32  
33  
34 using the GraphPad Prism 7.0 software package, where  $[\text{I}]$  is the concentration of a PAD.  
35  
36  
37  
38  
39  
40  
41

### 42 **Time dependent inactivation of citrullinated NNMT**

43  
44  
45 Time dependent NNMT citrullination was carried out as described above. Aliquots were  
46  
47 removed at various time intervals (0, 15, 30, 45, 60, 75, 90, 105, and 120 min) and assayed for  
48  
49 methyltransferase activity as described above. The experiment was carried out in duplicate, the  
50  
51 data plotted as a function of time and were fit to equation 4,  
52  
53

$$A = A_0 e^{-kt} \quad \text{Eq 4,}$$

1  
2  
3 using the GraphPad Prism 7.0 software package.  $A$  is the percent activity and  $A_0$  is the percent  
4 activity at time zero.  $k$  is the pseudo-first order rate constant of inactivation of citrullinated  
5 NNMT and  $t$  is time.  
6  
7  
8  
9  
10  
11  
12

### 13 **Steady-state kinetics of PAD1 and PAD2 with NNMT as a substrate.**

14  
15  
16 For kinetic measurements, a standard curve was generated with different concentrations of  
17 citrullinated histone H3. Briefly, histone H3 (100  $\mu\text{M}$ ) was treated with PAD4 (0.2  $\mu\text{M}$ ) in  
18 reaction buffer at 37  $^\circ\text{C}$  for 1 h. Samples were then treated with 20% TCA and 0.1 mM Rh-PG  
19 at 37  $^\circ\text{C}$  for 30 min. All samples were quenched with citrulline, cooled, centrifuged, washed and  
20 dried, as described above. After resuspending in 50 mM HEPES, samples were separated by  
21 SDS-PAGE (15%; 170 V; 50 min) and imaged on a Typhoon scanner (approximate  
22 excitation/emission maxima  $\sim 546/579$ , respectively). Images were analyzed using ImageJ and  
23 the band intensities fit to equation 5,  
24  
25  
26  
27  
28  
29  
30  
31  
32  
33

$$34 \quad y = mx + c \quad \text{Eq 5,}$$

35 where  $m$  is the slope of the line and  $c$  is the intercept.  
36  
37  
38

39 For the kinetic assay, varying concentrations of both NNMT (0, 0.375, 0.75, 1.5, 3, 6, and  
40 12  $\mu\text{M}$ ) were treated with PAD1 (0.2  $\mu\text{M}$ ) or PAD2 (0.4  $\mu\text{M}$ ) in reaction buffer at 37  $^\circ\text{C}$  for 20  
41 min. Reactions were then treated with 20% TCA and 0.1 mM Rh-PG at 37  $^\circ\text{C}$  for 30 min. All  
42 samples were quenched with citrulline, cooled, centrifuged, washed and dried as described  
43 above. After resuspending in 20 mM HEPES pH 8.0, 100 mM arginine, 1% SDS, 7%  $\beta$ -  
44 mercapto ethanol, and 100 mM NaCl. Samples were separated by SDS-PAGE and imaged on a  
45 Typhoon scanner (approximate excitation/emission maxima  $\sim 546/579$ , respectively). Images  
46  
47  
48  
49  
50  
51  
52  
53  
54  
55  
56  
57  
58  
59  
60

1  
2  
3 were analyzed using ImageJ and the initial rates fit to equation 1 using the GraphPad Prism 7.0  
4 software package. The experiment was carried out in duplicate.  
5  
6  
7  
8  
9  
10

## 11 **CD measurements**

12  
13  
14 CD measurements were carried out on a Jasco Model J-810 spectropolarimeter equipped  
15 with a thermoelectric temperature control system in a 1 cm cuvette (Hellma). Using a 1 cm path  
16 length and a 2.5 nm bandwidth, the data were in wavelength scanning mode, recording every 1  
17 nm from 215 to 265 nm, with an 8 s averaging time. For sample preparation, NNMT or the  
18 R132K mutant (5  $\mu$ M), treated with or without PAD1 (0.1  $\mu$ M), were incubated at 37  $^{\circ}$ C for 2 h  
19 (50 mM HEPES pH 7.6, 500  $\mu$ M TCEP, and 1 mM  $\text{CaCl}_2$ ). As a control, NNMT or the R132K  
20 mutant (5  $\mu$ M) were used directly without any incubation at 37  $^{\circ}$ C for 2 h. All samples were  
21 filtered through a 0.2  $\mu$ M filter to remove any aggregates and the samples were diluted to 2  $\mu$ M  
22 for recording CD spectra. The Bradford assay was used to determine protein concentrations.  
23 Data obtained for PAD1 alone was subtracted from the PAD1 treated samples. Final data was  
24 converted to molar ellipticity using equation 6,  
25  
26  
27  
28  
29  
30  
31  
32  
33  
34  
35  
36  
37  
38

$$39 \quad [\theta]_{\lambda} = (\text{MRW} \cdot \theta_{\lambda}) / (10 \cdot d \cdot c) \quad \text{Eq}$$

40  
41  
42 **6,**

43 where MRW is the mean residue ellipticity, c is the concentration in g/mL and d is the pathlength  
44 in cm.  
45  
46  
47  
48  
49  
50  
51  
52  
53  
54  
55  
56  
57  
58  
59  
60

1  
2  
3  
4  
5  
6  
7  
8  
9  
10  
11  
12  
13  
14  
15  
16  
17  
18  
19  
20  
21  
22  
23  
24  
25  
26  
27  
28  
29  
30  
31  
32  
33  
34  
35  
36  
37  
38  
39  
40  
41  
42  
43  
44  
45  
46  
47  
48  
49  
50  
51  
52  
53  
54  
55  
56  
57  
58  
59  
60

1  
2  
3 **ASSOCIATED CONTENT**  
4

5 **Supporting information.** Table S1, S2, and S3, and Figures S1-S9. This information is  
6 available free of charge via the Internet at <http://pubs.acs.org>.  
7  
8

9  
10 **AUTHOR INFORMATION**  
11

12 **Corresponding Author.** \*Tel.: (508)-856-8492. Fax: 508-856-6215. E-mail:  
13 [paul.thompson@umassmed.edu](mailto:paul.thompson@umassmed.edu).  
14

15  
16  
17 ORCID ID:

18  
19 Paul R. Thompson: 0000-0002-1621-3372

20  
21 Venkatesh V. Nemmara – ORCID ID - 0000-0001-6925-869X  
22

23  
24 **ACKNOWLEDGEMENTS**  
25

26 This work was supported in part by NIH grant GM109767 (P.R.T.). We would like to thank  
27  
28 R.C. Mathews and R. Jain for their help with the CD experiments.  
29  
30  
31  
32  
33  
34  
35  
36  
37  
38  
39  
40  
41  
42  
43  
44  
45  
46  
47  
48  
49  
50  
51  
52  
53  
54  
55  
56  
57  
58  
59  
60



**ABBREVIATIONS**

RA, Rheumatoid arthritis; PAD, Protein arginine deiminase; ACPA, Anti-citrullinated protein antibodies; TCA, trichloroacetic acid; NNMT, Nicotinamide-N-methyl transferase; NAM, nicotinamide; MeNAM, N-methyl nicotinamide; ASO, Antisense oligonucleotides.

**References.**

- (1) Rini, J., Szumlanski, C., Guercioli, R., and Weinshilboum, R. M. (1990) Human liver nicotinamide N-methyltransferase: ion-pairing radiochemical assay, biochemical properties and individual variation, *Clin Chim Acta* **186**, 359-374.
- (2) Aksoy, S., Szumlanski, C. L., and Weinshilboum, R. M. (1994) Human liver nicotinamide N-methyltransferase. cDNA cloning, expression, and biochemical characterization, *J Biol Chem* **269**, 14835-14840.
- (3) Cantoni, G. L. (1951) Methylation of nicotinamide with soluble enzyme system from rat liver, *J Biol Chem* **189**, 203-216.
- (4) Kraus, D., Yang, Q., Kong, D., Banks, A. S., Zhang, L., Rodgers, J. T., Pirinen, E., Pulinilkunnil, T. C., Gong, F., Wang, Y. C., Cen, Y., Sauve, A. A., Asara, J. M., Peroni, O. D., Monia, B. P., Bhanot, S., Alhonen, L., Puigserver, P., and Kahn, B. B. (2014) Nicotinamide N-methyltransferase knockdown protects against diet-induced obesity, *Nature* **508**, 258-262.
- (5) Alston, T. A., and Abeles, R. H. (1988) Substrate specificity of nicotinamide methyltransferase isolated from porcine liver, *Arch Biochem Biophys* **260**, 601-608.
- (6) Yan, L., Otterness, D. M., Craddock, T. L., and Weinshilboum, R. M. (1997) Mouse liver nicotinamide N-methyltransferase: cDNA cloning, expression, and nucleotide sequence polymorphisms, *Biochem Pharmacol* **54**, 1139-1149.
- (7) Riederer, M., Erwa, W., Zimmermann, R., Frank, S., and Zechner, R. (2009) Adipose tissue as a source of nicotinamide N-methyltransferase and homocysteine, *Atherosclerosis* **204**, 412-417.

- 1  
2  
3 (8) Xu, J., Moatamed, F., Caldwell, J. S., Walker, J. R., Kraiem, Z., Taki, K., Brent, G. A., and Hershman, J.  
4  
5 M. (2003) Enhanced expression of nicotinamide N-methyltransferase in human papillary thyroid  
6  
7 carcinoma cells, *J Clin Endocrinol Metab* 88, 4990-4996.  
8  
9  
10 (9) Xu, J., Capezzone, M., Xu, X., and Hershman, J. M. (2005) Activation of nicotinamide N-  
11  
12 methyltransferase gene promoter by hepatocyte nuclear factor-1beta in human papillary  
13  
14 thyroid cancer cells, *Mol Endocrinol* 19, 527-539.  
15  
16  
17 (10) Chen, C., Wang, X., Huang, X., Yong, H., Shen, J., Tang, Q., Zhu, J., Ni, J., and Feng, Z. (2016)  
18  
19 Nicotinamide N-methyltransferase: a potential biomarker for worse prognosis in gastric  
20  
21 carcinoma, *Am J Cancer Res* 6, 649-663.  
22  
23  
24 (11) Sartini, D., Muzzonigro, G., Milanese, G., Pierella, F., Rossi, V., and Emanuelli, M. (2006)  
25  
26 Identification of nicotinamide N-methyltransferase as a novel tumor marker for renal clear cell  
27  
28 carcinoma, *J Urol* 176, 2248-2254.  
29  
30  
31 (12) Tang, S. W., Yang, T. C., Lin, W. C., Chang, W. H., Wang, C. C., Lai, M. K., and Lin, J. Y. (2011)  
32  
33 Nicotinamide N-methyltransferase induces cellular invasion through activating matrix  
34  
35 metalloproteinase-2 expression in clear cell renal cell carcinoma cells, *Carcinogenesis* 32, 138-  
36  
37 145.  
38  
39  
40 (13) Mobley, A., Zhang, S., Bondaruk, J., Wang, Y., Majewski, T., Caraway, N. P., Huang, L., Shoshan, E.,  
41  
42 Velazquez-Torres, G., Nitti, G., Lee, S., Lee, J. G., Fuentes-Mattei, E., Willis, D., Zhang, L., Guo, C.  
43  
44 C., Yao, H., Baggerly, K., Lotan, Y., Lerner, S. P., Dinney, C., McConkey, D., Bar-Eli, M., and  
45  
46 Czerniak, B. (2017) Aurora Kinase A is a Biomarker for Bladder Cancer Detection and Contributes  
47  
48 to its Aggressive Behavior, *Sci Rep* 7, 40714.  
49  
50  
51  
52  
53  
54  
55  
56  
57  
58  
59  
60

- 1  
2  
3 (14) Fahrman, J. F., Grapov, D. D., Wanichthanarak, K., DeFelice, B. C., Salemi, M. R., Rom, W. N.,  
4  
5 Gandara, D. R., Phinney, B. S., Fiehn, O., Pass, H., and Miyamoto, S. (2017) Integrated  
6  
7 Metabolomics and Proteomics Highlight Altered Nicotinamide- and Polyamine Pathways in Lung  
8  
9 Adenocarcinoma, *Carcinogenesis* DOI: 10.1093/carcin/bgw205.  
10  
11  
12 (15) Palanichamy, K., Kanji, S., Gordon, N., Thirumoorthy, K., Jacob, J. R., Litzenberg, K. T., Patel, D., and  
13  
14 Chakravarti, A. (2017) NNMT Silencing Activates Tumor Suppressor PP2A, Inactivates Oncogenic  
15  
16 STKs, and Inhibits Tumor Forming Ability, *Clin Cancer Res* 23, 2325-2334.  
17  
18  
19 (16) Roessler, M., Rollinger, W., Palme, S., Hagmann, M. L., Berndt, P., Engel, A. M., Schneidinger, B.,  
20  
21 Pfeffer, M., Andres, H., Karl, J., Bodenmuller, H., Ruschoff, J., Henkel, T., Rohr, G., Rossol, S.,  
22  
23 Rosch, W., Langen, H., Zolg, W., and Tacke, M. (2005) Identification of nicotinamide N-  
24  
25 methyltransferase as a novel serum tumor marker for colorectal cancer, *Clin Cancer Res* 11,  
26  
27 6550-6557.  
28  
29  
30 (17) Tomida, M., Mikami, I., Takeuchi, S., Nishimura, H., and Akiyama, H. (2009) Serum levels of  
31  
32 nicotinamide N-methyltransferase in patients with lung cancer, *J Cancer Res Clin Oncol* 135,  
33  
34 1223-1229.  
35  
36  
37 (18) Parsons, R. B., Smith, S. W., Waring, R. H., Williams, A. C., and Ramsden, D. B. (2003) High  
38  
39 expression of nicotinamide N-methyltransferase in patients with idiopathic Parkinson's disease,  
40  
41 *Neurosci Lett* 342, 13-16.  
42  
43  
44 (19) Aoyama, K., Matsubara, K., Kondo, M., Murakawa, Y., Suno, M., Yamashita, K., Yamaguchi, S., and  
45  
46 Kobayashi, S. (2001) Nicotinamide-N-methyltransferase is higher in the lumbar cerebrospinal  
47  
48 fluid of patients with Parkinson's disease, *Neurosci Lett* 298, 78-80.  
49  
50  
51  
52  
53  
54  
55  
56  
57  
58  
59  
60

- 1  
2  
3 (20) Cao, Y., Matsubara, T., Zhao, C., Gao, W., Peng, L., Shan, J., Liu, Z., Yuan, F., Tang, L., Li, P., Guan, Z.,  
4 Fang, Z., Lu, X., Huang, H., and Yang, Q. (2017) Antisense oligonucleotide and thyroid hormone  
5 conjugates for obesity treatment, *Sci Rep* 7, 9307.  
6  
7  
8  
9  
10 (21) Ulanovskaya, O. A., Zuhl, A. M., and Cravatt, B. F. (2013) NNMT promotes epigenetic remodeling in  
11 cancer by creating a metabolic methylation sink, *Nat Chem Biol* 9, 300-306.  
12  
13  
14  
15 (22) Perkins, N. D. (2006) Post-translational modifications regulating the activity and function of the  
16 nuclear factor kappa B pathway, *Oncogene* 25, 6717-6730.  
17  
18  
19  
20 (23) Walsh, G., and Jefferis, R. (2006) Post-translational modifications in the context of therapeutic  
21 proteins, *Nat Biotechnol* 24, 1241-1252.  
22  
23  
24  
25 (24) Lim, B. H., Cho, B. I., Kim, Y. N., Kim, J. W., Park, S. T., and Lee, C. W. (2006) Overexpression of  
26 nicotinamide N-methyltransferase in gastric cancer tissues and its potential post-translational  
27 modification, *Exp Mol Med* 38, 455-465.  
28  
29  
30  
31  
32 (25) Tilwawala, R., Nguyen, S. H., Maurais, A. J., Nemmara, V. V., Nagar, M., Salinger, A. J., Nagpal, S.,  
33 Weerapana, E., and Thompson, P. R. (2018) The Rheumatoid Arthritis-Associated Citrullinome,  
34 *Cell Chem Biol* 25, 691-704.  
35  
36  
37  
38  
39 (26) Fuhrmann, J., Clancy, K. W., and Thompson, P. R. (2015) Chemical biology of protein arginine  
40 modifications in epigenetic regulation, *Chem Rev* 115, 5413-5461.  
41  
42  
43  
44 (27) Nemmara, V. V., Subramanian, V., Muth, A., Mondal, S., Salinger, A. J., Maurais, A. J., Tilwawala, R.,  
45 Weerapana, E., and Thompson, P. R. (2018) The Development of Benzimidazole-Based Clickable  
46 Probes for the Efficient Labeling of Cellular Protein Arginine Deiminases (PADs), *ACS Chem Biol*  
47 *13*, 712-722.  
48  
49  
50  
51  
52  
53  
54  
55  
56  
57  
58  
59  
60

- 1  
2  
3 (28) Zhang, X., Liu, X., Zhang, M., Li, T., Muth, A., Thompson, P. R., Coonrod, S. A., and Zhang, X. (2016)  
4  
5 Peptidylarginine deiminase 1-catalyzed histone citrullination is essential for early embryo  
6  
7 development, *Sci Rep* 6, 38727.  
8  
9
- 10 (29) Zhang, X., Bolt, M., Guertin, M. J., Chen, W., Zhang, S., Cherrington, B. D., Slade, D. J., Dreyton, C. J.,  
11  
12 Subramanian, V., Bicker, K. L., Thompson, P. R., Mancini, M. A., Lis, J. T., and Coonrod, S. A.  
13  
14 (2012) Peptidylarginine deiminase 2-catalyzed histone H3 arginine 26 citrullination facilitates  
15  
16 estrogen receptor alpha target gene activation, *Proc Natl Acad Sci U S A* 109, 13331-13336.  
17  
18
- 19 (30) Bicker, K. L., and Thompson, P. R. (2013) The protein arginine deiminases: Structure, function,  
20  
21 inhibition, and disease, *Biopolymers* 99, 155-163.  
22  
23  
24
- 25 (31) Jones, J. E., Causey, C. P., Knuckley, B., Slack-Noyes, J. L., and Thompson, P. R. (2009) Protein  
26  
27 arginine deiminase 4 (PAD4): Current understanding and future therapeutic potential, *Curr Opin*  
28  
29 *Drug Discov Devel* 12, 616-627.  
30  
31
- 32 (32) Esposito, G., Vitale, A. M., Leijten, F. P., Strik, A. M., Koonen-Reemst, A. M., Yurttas, P., Robben, T.  
33  
34 J., Coonrod, S., and Gossen, J. A. (2007) Peptidylarginine deiminase (PAD) 6 is essential for  
35  
36 oocyte cytoskeletal sheet formation and female fertility, *Mol Cell Endocrinol* 273, 25-31.  
37  
38  
39
- 40 (33) Senshu, T., Kan, S., Ogawa, H., Manabe, M., and Asaga, H. (1996) Preferential deimination of  
41  
42 keratin K1 and filaggrin during the terminal differentiation of human epidermis, *Biochem*  
43  
44 *Biophys Res Commun* 225, 712-719.  
45  
46
- 47 (34) Qin, H., Liu, X., Li, F., Miao, L., Li, T., Xu, B., An, X., Muth, A., Thompson, P. R., Coonrod, S. A., and  
48  
49 Zhang, X. (2017) PAD1 promotes epithelial-mesenchymal transition and metastasis in triple-  
50  
51 negative breast cancer cells by regulating MEK1-ERK1/2-MMP2 signaling, *Cancer Lett* 409, 30-  
52  
53 41.  
54  
55  
56  
57

- 1  
2  
3 (35) Mohanan, S., Cherrington, B. D., Horibata, S., McElwee, J. L., Thompson, P. R., and Coonrod, S. A.  
4  
5 (2012) Potential role of peptidylarginine deiminase enzymes and protein citrullination in cancer  
6  
7 pathogenesis, *Biochem Res Int* 2012, 895343.  
8  
9  
10 (36) McElwee, J. L., Mohanan, S., Griffith, O. L., Breuer, H. C., Anguish, L. J., Cherrington, B. D., Palmer,  
11  
12 A. M., Howe, L. R., Subramanian, V., Causey, C. P., Thompson, P. R., Gray, J. W., and Coonrod, S.  
13  
14 A. (2012) Identification of PADI2 as a potential breast cancer biomarker and therapeutic target,  
15  
16 *BMC Cancer* 12, 500.  
17  
18  
19 (37) Damgaard, D., Senolt, L., Nielsen, M. F., Pruijn, G. J., and Nielsen, C. H. (2014) Demonstration of  
20  
21 extracellular peptidylarginine deiminase (PAD) activity in synovial fluid of patients with  
22  
23 rheumatoid arthritis using a novel assay for citrullination of fibrinogen, *Arthritis Res Ther* 16,  
24  
25 498.  
26  
27  
28 (38) Burska, A. N., Hunt, L., Boissinot, M., Stollo, R., Ryan, B. J., Vital, E., Nissim, A., Winyard, P. G.,  
29  
30 Emery, P., and Ponchel, F. (2014) Autoantibodies to posttranslational modifications in  
31  
32 rheumatoid arthritis, *Mediators Inflamm* 2014, 492873.  
33  
34  
35 (39) Muth, A., Subramanian, V., Beaumont, E., Nagar, M., Kerry, P., McEwan, P., Srinath, H., Clancy, K.,  
36  
37 Parelkar, S., and Thompson, P. R. (2017) Development of a Selective Inhibitor of Protein Arginine  
38  
39 Deiminase 2, *J Med Chem* 60, 3198-3211.  
40  
41  
42 (40) Mondal, S., Parelkar, S. S., Nagar, M., and Thompson, P. R. (2018) Photochemical Control of Protein  
43  
44 Arginine Deiminase (PAD) Activity, *ACS Chem Biol* 13, 1057-1065.  
45  
46  
47 (41) van Haren, M. J., Sastre Torano, J., Sartini, D., Emanuelli, M., Parsons, R. B., and Martin, N. I. (2016)  
48  
49 A Rapid and Efficient Assay for the Characterization of Substrates and Inhibitors of Nicotinamide  
50  
51 N-Methyltransferase, *Biochemistry* 55, 5307-5315.  
52  
53  
54  
55  
56  
57  
58  
59  
60

- 1  
2  
3 (42) Neelakantan, H., Vance, V., Wang, H. L., McHardy, S. F., and Watowich, S. J. (2017) Noncoupled  
4  
5       Fluorescent Assay for Direct Real-Time Monitoring of Nicotinamide N-Methyltransferase  
6  
7       Activity, *Biochemistry* 56, 824-832.  
8  
9
- 10 (43) Bicker, K. L., Subramanian, V., Chumanevich, A. A., Hofseth, L. J., and Thompson, P. R. (2012) Seeing  
11  
12       citrulline: development of a phenylglyoxal-based probe to visualize protein citrullination, *J Am*  
13  
14       *Chem Soc* 134, 17015-17018.  
15  
16  
17
- 18 (44) Knuckley, B., Causey, C. P., Jones, J. E., Bhatia, M., Dreyton, C. J., Osborne, T. C., Takahara, H., and  
19  
20       Thompson, P. R. (2010) Substrate specificity and kinetic studies of PADs 1, 3, and 4 identify  
21  
22       potent and selective inhibitors of protein arginine deiminase 3, *Biochemistry* 49, 4852-4863.  
23  
24
- 25 (45) Clancy, K. W., Weerapana, E., and Thompson, P. R. (2016) Detection and identification of protein  
26  
27       citrullination in complex biological systems, *Curr Opin Chem Biol* 30, 1-6.  
28  
29
- 30 (46) Lewallen, D. M., Bicker, K. L., Subramanian, V., Clancy, K. W., Slade, D. J., Martell, J., Dreyton, C. J.,  
31  
32       Sokolove, J., Weerapana, E., and Thompson, P. R. (2015) Chemical Proteomic Platform To  
33  
34       Identify Citrullinated Proteins, *ACS Chem Biol* 10, 2520-2528.  
35  
36  
37
- 38 (47) Choi, M., Song, J. S., Kim, H. J., Cha, S., and Lee, E. Y. (2013) Matrix-assisted laser desorption  
39  
40       ionization-time of flight mass spectrometry identification of peptide citrullination site using Br  
41  
42       signature, *Anal Biochem* 437, 62-67.  
43  
44
- 45 (48) Kozbial, P. Z., and Mushegian, A. R. (2005) Natural history of S-adenosylmethionine-binding  
46  
47       proteins, *BMC Struct Biol* 5, 19.  
48  
49
- 50 (49) Martin, J. L., and McMillan, F. M. (2002) SAM (dependent) I AM: the S-adenosylmethionine-  
51  
52       dependent methyltransferase fold, *Curr Opin Struct Biol* 12, 783-793.  
53  
54  
55  
56  
57



- 1  
2  
3 (50) Schubert, H. L., Blumenthal, R. M., and Cheng, X. (2003) Many paths to methyltransfer: a chronicle  
4 of convergence, *Trends Biochem Sci* 28, 329-335.  
5  
6  
7  
8 (51) Peng, Y., Sartini, D., Pozzi, V., Wilk, D., Emanuelli, M., and Yee, V. C. (2011) Structural basis of  
9 substrate recognition in human nicotinamide N-methyltransferase, *Biochemistry* 50, 7800-7808.  
10  
11  
12  
13 (52) Horibata, S., Rogers, K. E., Sadegh, D., Anguish, L. J., McElwee, J. L., Shah, P., Thompson, P. R., and  
14 Coonrod, S. A. (2017) Role of peptidylarginine deiminase 2 (PAD2) in mammary carcinoma cell  
15 migration, *BMC Cancer* 17, 378.  
16  
17  
18  
19  
20  
21 (53) Causey, C. P., Jones, J. E., Slack, J. L., Kamei, D., Jones, L. E., Subramanian, V., Knuckley, B., Ebrahimi,  
22 P., Chumanevich, A. A., Luo, Y., Hashimoto, H., Sato, M., Hofseth, L. J., and Thompson, P. R.  
23 (2011) The Development of N-alpha-(2-Carboxyl)benzoyl-N(5)-(2-fluoro-1-iminoethyl)-l-  
24 ornithine Amide (o-F-amidine) and N-alpha-(2-Carboxyl)benzoyl-N(5)-(2-chloro-1-iminoethyl)-l-  
25 ornithine Amide (o-Cl-amidine) As Second Generation Protein Arginine Deiminase (PAD)  
26 Inhibitors, *J Med Chem* 54, 6919-6935.  
27  
28  
29  
30  
31  
32  
33  
34  
35  
36  
37  
38  
39  
40  
41  
42  
43  
44  
45  
46  
47  
48  
49  
50  
51  
52  
53  
54  
55  
56  
57  
58  
59  
60

## Tables

Table 1. Comparison of the rate of citrullination of NNMT mutants with their rate of inactivation.

Proteins	Rate of	Rate of NNMT	Rate of NNMT
	citrullination	inactivation	inactivation
		with PAD1	No PAD1
	$k_{\text{obs}} \times 10^{-2} \text{ (min}^{-1}\text{)}$	$k_{\text{obs}} \times 10^{-2} \text{ (min}^{-1}\text{)}$	$k_{\text{obs}} \times 10^{-2} \text{ (min}^{-1}\text{)}$
NNMT	$4.0 \pm 0.1$	$1.6 \pm 0.1$	$0.10 \pm 0.03$
R18K	$4.8 \pm 0.6$	$2.3 \pm 0.1$	$0.30 \pm 0.06$
R132K	$5.0 \pm 0.3$	$0.9 \pm 0.1$	$1.2 \pm 0.1$
R181K	$4.0 \pm 0.2$	$1.6 \pm 0.2$	$0.18 \pm 0.03$

**Figures Legends.**

**Figure 1.** (A) NNMT catalyzed methylation of nicotinamide (NAM) to *N*-methylnicotinamide (MeNAM) in the presence of *S*-adenosylmethionine (SAM). (B) PAD-catalyzed hydrolysis of peptidyl-arginine to peptidyl-citrulline. (C) Fold change in the  $k_{\text{cat}}/K_{\text{M}}$  of wild type NNMT (citrullinated/uncitrullinated) after treatment with PAD1, 2, 3, or 4.

**Figure 2.** (A) Time dependent citrullination of NNMT by PAD1 and PAD2 visualized by Rh-PG labeling. (B) Time courses of NNMT citrullination by PAD1 and PAD2 visualized by Rh-PG labeling. The data were fit to eq 2 (see methods). (C) Concentration dependent citrullination of NNMT by PAD1 and PAD2 visualized by Rh-PG labeling. (D) Michaelis-Menten plot showing the activity of PAD1 and PAD2 against NNMT.

**Figure 3.** (A) Workflow showing the labeling of citrullinated NNMT by phenylglyoxal and subsequent digestion with neutrophil elastase for the mass spectrometric detection of citrullinated peptides. (B) Table showing citrullinated peptides detected by mass spectrometry. Citrullinated residues are marked by an asterisk. The citrullinated residue number in NNMT is shown in the first column. (C) Representative MS/MS spectrum showing phenylglyoxal labeled NNMT at residue 132, which is citrullinated by PAD2.

**Figure 4.** (A) Ribbon representation (in green) of NNMT showing arginine residues in red (PDB code 3ROD). (B) Activity of NNMT and mutants measured using quinoline and SAM as

1  
2  
3 substrates. (C) Time dependent citrullination of NNMT by PAD1 and PAD2 visualized by Rh-  
4 PG labeling. (D) Time courses of NNMT citrullination by PAD1 and PAD2 visualized by Rh-PG  
5 labeling. The data were fit to eq 2 (see methods). (E) Comparison of time dependent inactivation  
6 of WT and R132K as a result of PAD1 mediated citrullination. (F) Comparison of time  
7 dependent inactivation of R18K and R181K as a result of PAD1 mediated citrullination.  
8  
9  
10  
11  
12  
13  
14  
15  
16  
17

18 **Figure 5.** (A) Ribbon structure of NNMT highlighting the active site loop (sienna) and helix 1  
19 (purple). The residues in the loop and the helix interact with the cofactor SAM and are proposed  
20 to be essential for its binding at the active site. (B) Ribbon representation of NNMT depicting the  
21 interaction of R132 with W97 and E128. (C) CD spectra of citrullinated and uncitrullinated  
22 NNMT at 37 °C. The spectra of NNMT without incubation is shown for reference. (D) CD  
23 spectra of citrullinated and uncitrullinated NNMT-R132K at 37 °C. The spectra of NNMT  
24 without incubation is shown for reference.  
25  
26  
27  
28  
29  
30  
31  
32  
33  
34  
35  
36  
37  
38  
39  
40  
41  
42  
43  
44  
45  
46  
47  
48  
49  
50  
51  
52  
53  
54  
55  
56  
57  
58  
59  
60

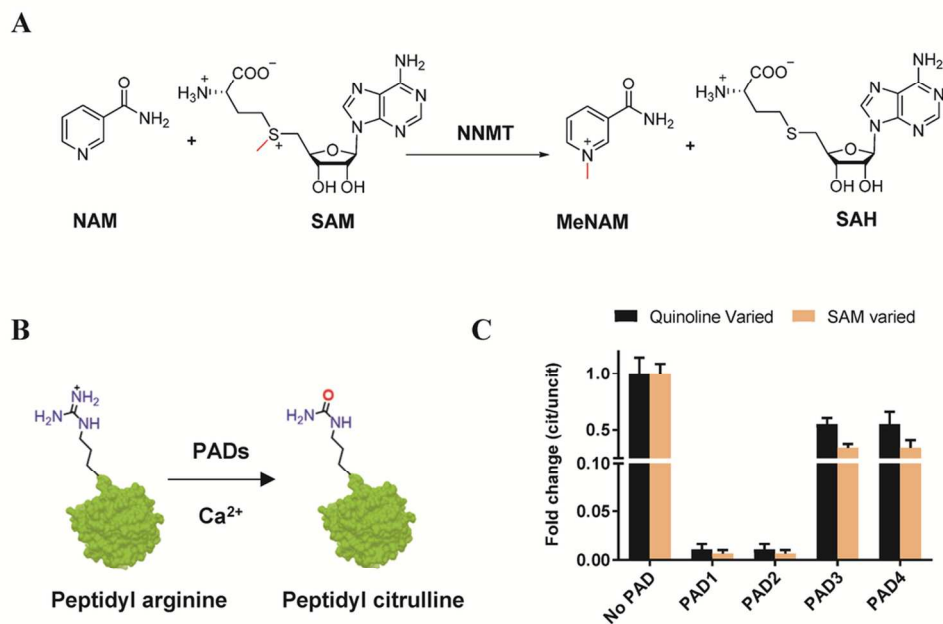


Figure 1. (A) NNMT catalyzed methylation of nicotinamide (NAM) to N-methylnicotinamide (MeNAM) in the presence of S-adenosylmethionine (SAM). (B) PAD-catalyzed hydrolysis of peptidyl-arginine to peptidyl-citrulline. (C) Fold change in the  $k_{cat}/K_M$  of wild type NNMT (citrullinated/uncitrullinated) after treatment with PAD1, 2, 3, or 4.

98x66mm (300 x 300 DPI)

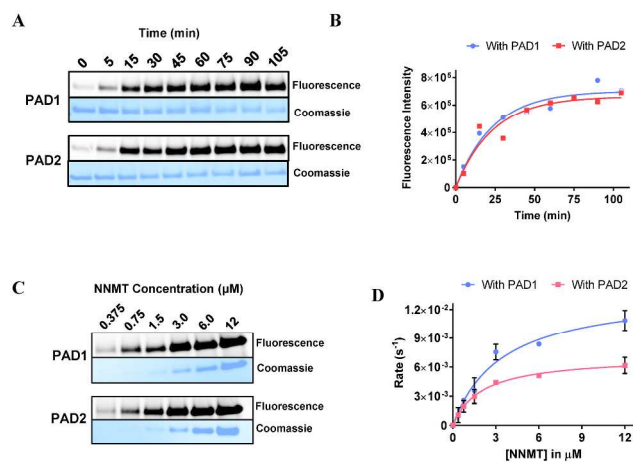


Figure 2. (A) Time dependent citrullination of NNMT by PAD1 and PAD2 visualized by Rh-PG labeling. (B) Time courses of NNMT citrullination by PAD1 and PAD2 visualized by Rh-PG labeling. The data were fit to eq 2 (see methods). (C) Concentration dependent citrullination of NNMT by PAD1 and PAD2 visualized by Rh-PG labeling. (D) Michaelis-Menten plot showing the activity of PAD1 and PAD2 against NNMT.

279x361mm (300 x 300 DPI)

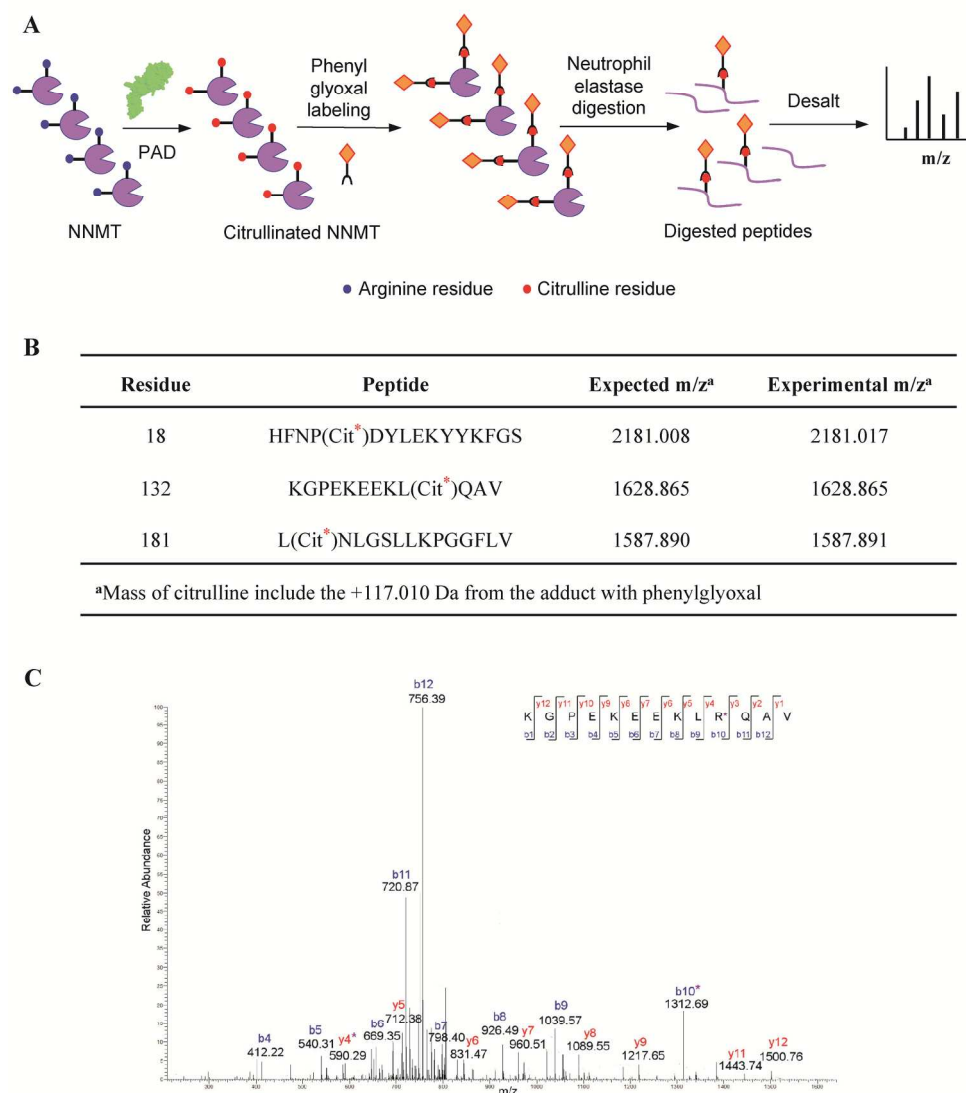


Figure 3. (A) Workflow showing the labeling of citrullinated NNMT by phenylglyoxal and subsequent digestion with neutrophil elastase for the mass spectrometric detection of citrullinated peptides. (B) Table showing citrullinated peptides detected by mass spectrometry. Citrullinated residues are marked by an asterisk. The citrullinated residue number in NNMT is shown in the first column. (C) Representative MS/MS spectrum showing phenylglyoxal labeled NNMT at residue 132, which is citrullinated by PAD2.

193x219mm (300 x 300 DPI)

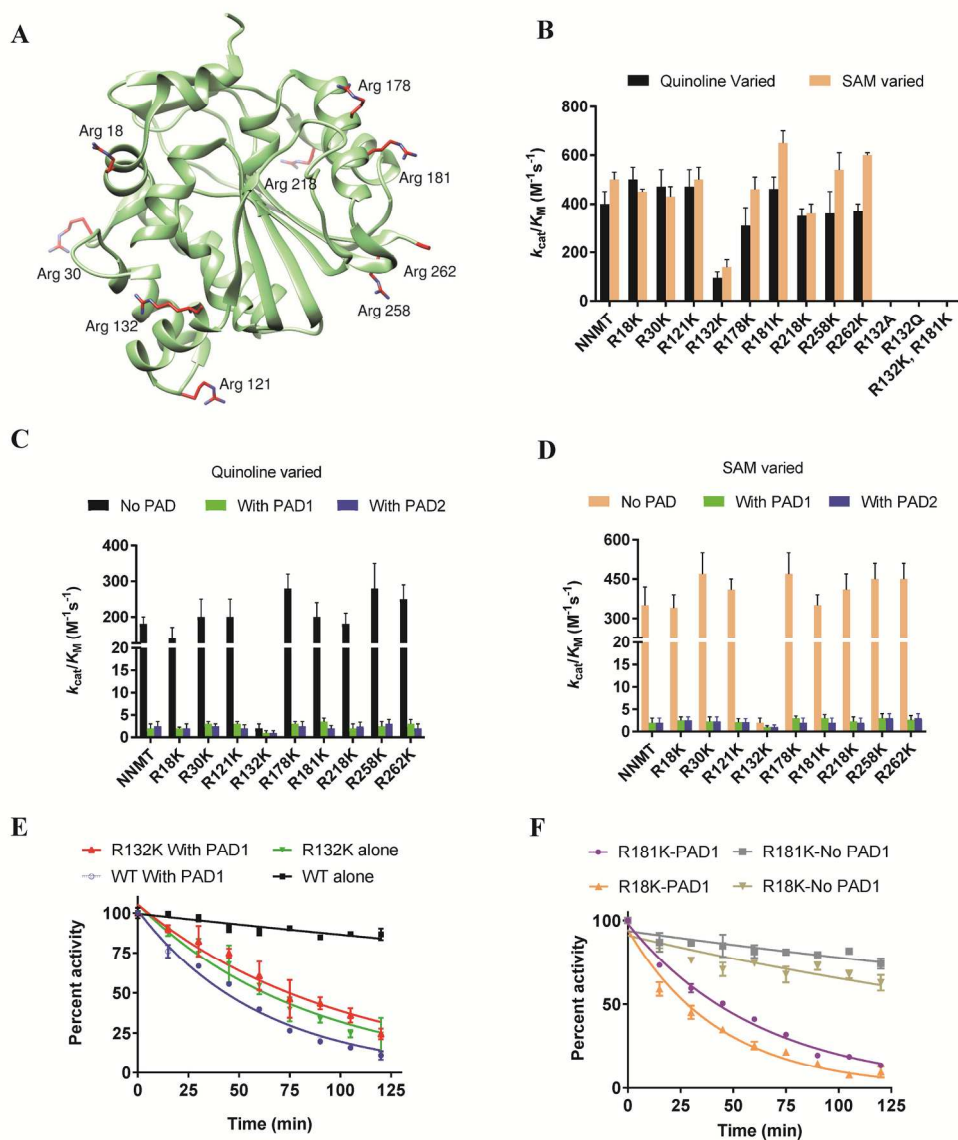


Figure 4. (A) Ribbon representation (in green) of NNMT showing arginine residues in red (PDB code 3ROD). (B) Activity of NNMT and mutants measured using quinoline and SAM as substrates. (C) Time dependent citrullination of NNMT by PAD1 and PAD2 visualized by Rh-PG labeling. (D) Time courses of NNMT citrullination by PAD1 and PAD2 visualized by Rh-PG labeling. The data were fit to eq 2 (see methods). (E) Comparison of time dependent inactivation of WT and R132K as a result of PAD1 mediated citrullination. (F) Comparison of time dependent inactivation of R18K and R181K as a result of PAD1 mediated citrullination.

186x218mm (300 x 300 DPI)



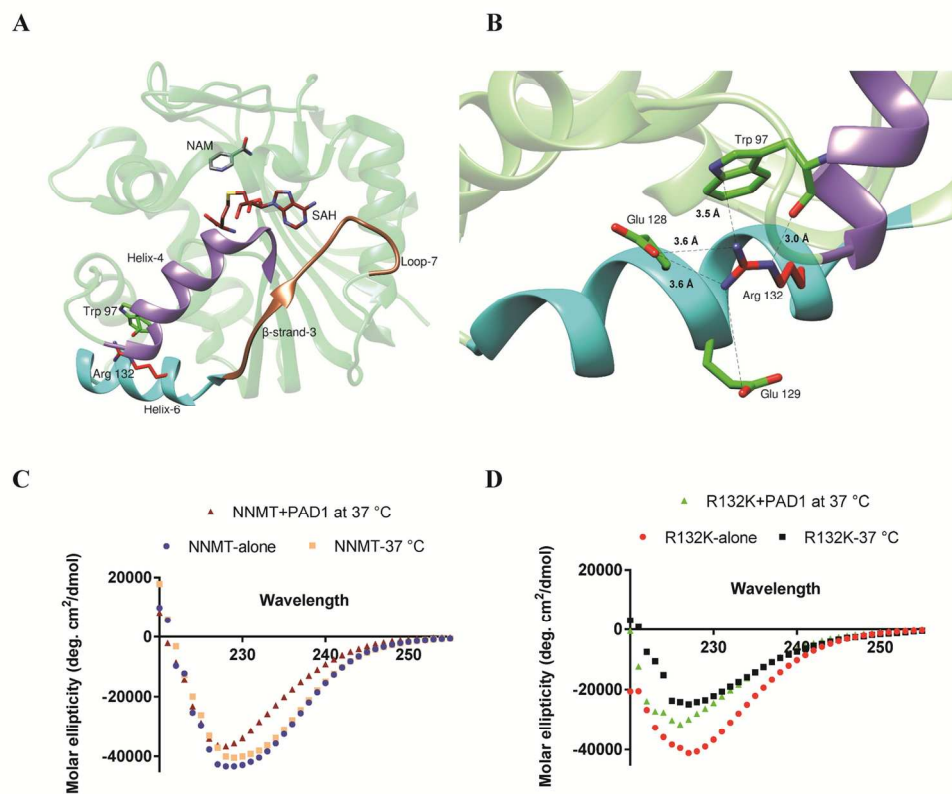
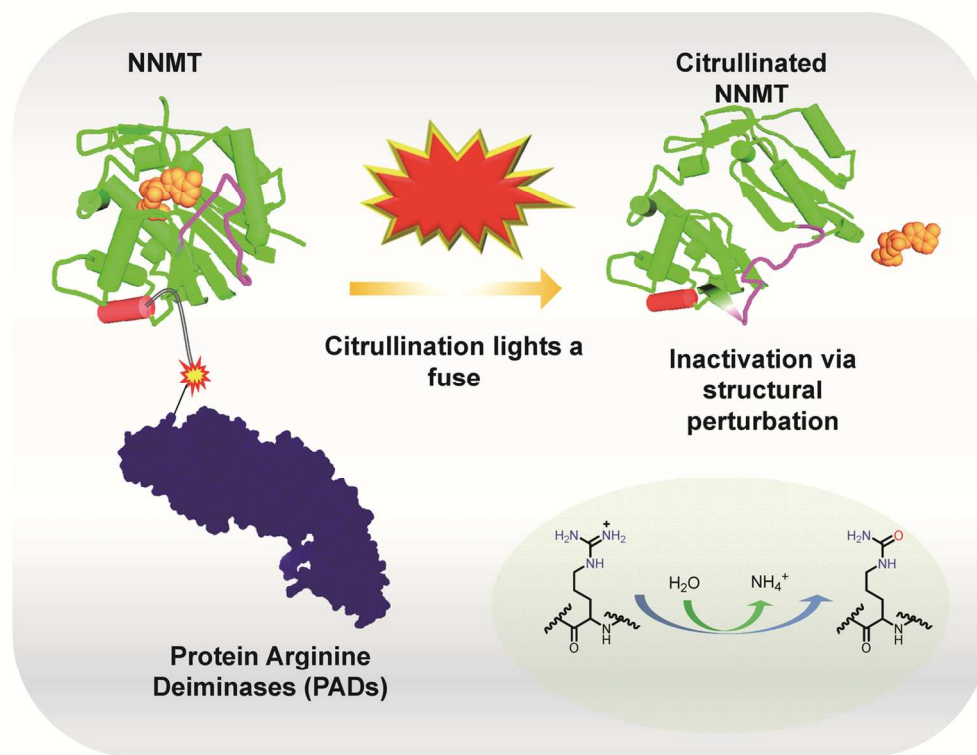


Figure 5. (A) Ribbon structure of NNMT highlighting the active site loop (sienna) and helix 1 (purple). The residues in the loop and the helix interact with the cofactor SAM and are proposed to be essential for its binding at the active site. (B) Ribbon representation of NNMT depicting the interaction of R132 with W97 and E128. (C) CD spectra of citrullinated and uncitrullinated NNMT at 37 °C. The spectra of NNMT without incubation is shown for reference. (D) CD spectra of citrullinated and uncitrullinated NNMT-R132K at 37 °C. The spectra of NNMT without incubation is shown for reference.

144x124mm (300 x 300 DPI)



TOC Graphic

124x94mm (300 x 300 DPI)